COBEM 2021 26th International Congress of Mechanical Engineering

ABCM Associação Brasileira de Engenharia e Ciências Mecânicas
November 22-26, 2021, Virtual Congress, Brazil

COB-2021-XXXX (XXXX is the identification number of the final paper) DETECTION OF SUBSEA GAS LEAKAGES VIA COMPUTATIONAL FLUID DYNAMICS AND CONVOLUTIONAL NEURAL NETWORKS

Gustavo Luís Rodrigues Caldas
School of Chemistry/Federal University of Rio de Janeiro. Av. Athos da Silveira Ramos, 149, Bloco E, Sl. 207. Ilha do Fundão - Rio de Janeiro, Brazil
gustavo.caldas@eq.ufrj.br

Thiago Bento
Federal Center for Technological Education Celso Suckow da Fonseca (Cefet/RJ)
tbento@id.uff.br

Roger Matsumoto Moreira
School of Engineering / Fluminense Federal University. Rua Passos da Patria, 156, bl.D, sl.563A. Niterói - Rio de Janeiro, Brazil
rmmoreira@id.uff.br

Maurício Bezerra de Souza Júnior
School of Chemistry/Federal University of Rio de Janeiro. Av. Athos da Silveira Ramos, 149, Bloco E, Sl. 207. Ilha do Fundão - Rio de Janeiro, Brazil
mbsj@eq.ufrj.br

Abstract. *Gas leakage can generate a considerable number of losses in environmental and economic terms. Constant monitoring of deep-water wells is an important safety tool to enable fast and proper responses, prevent the conditions' aggravation, and avoid unnecessary costs. A qualitative approach is to install video cameras in the subsea environment to track possible leaks. Automation of this process is possible by using image analyses algorithms. In this context, Convolutional neural network (CNN) is a methodology part of the Artificial Intelligence framework, capable of extracting relevant features from images. Therefore, the objective of this work is to develop a tool to detect fault in the subsea pipelines using the presence of bubbles in the images as an indicator. Computational Fluid Dynamics simulations were developed aiming to reproduce subsea gas leakages. The volume of fluid (VOF) method is employed to model the two-phase gas-liquid flow, in which bubbles are released into stagnant water with several velocities and from different pipelines orifice diameters. The frames obtained from the simulation images served as input to the CNN. The methodology is intended to distinguish between a scenario of normality (no leakage/bubble) and abnormality (leakage/bubble). The classification task of bubble presence or absence performed by the CNN reported high accuracy (99 %). No false alarms (fall-outs) in all sets and high specificity (true negative rate) and precision of the classifier were found. Good accuracy supports its potential as fault detector. It could be extended to other applications in the field of Fault Detection and Diagnosis, not only limiting to this scope.*

Keywords: *gas leakage, convolutional neural networks, subsea pipelines, CFD, fault detection.*

1. INTRODUCTION

Subsea oil well drilling activities and their transportation by pipelines are susceptible to incidents of significant environmental and economic impact, especially if in decommissioning state and/or after a long time of service (Nazir *et al.*, 2008). Olsen and Skjetne (2016) classify these incidents in seep, which could occur naturally or due to drilling activity; leaks, may not be detected if of small scale; rupture, an event of greater impact, but with control; blowout, a major release with loss of control. Eventually, cracks in these wells pipelines may evolve from small leaks to large material release. Containing the leakage on early stage can be the key to avoid a disaster. Therefore, the use of risk assessment techniques is justified, one of which is ROVs (remotely operated vehicles), which register these events *in loco*. With the leakage visualization, a fast and safe response can be performed, allowing the technicians a complete evaluation of the situation, especially for events that pose great danger.

Fault detection and diagnosis (FDD) have become a central point to the process industry because the ramping operations complexity demands loss prevention and environmental safety maintenance. In the FDD terminology, fault is a system state in which there is a deviation from the accepted operational range. It is important to note that detection denotes whether the fault has occurred, while diagnosis points out which fault is, its type, and its magnitude (Isermann, 2006; Chiang *et al.*, 2001). Venkatasubramanian divided the methods into three: quantitative model-based (Venkatasubramanian *et al.*, 2003b), qualitative models and search strategies (Venkatasubramanian *et al.*, 2003a), and process history based (Venkatasubramanian *et al.*, 2003c). One of the latter techniques is artificial neural networks (ANN), a data-driven approach that recognizes patterns without modelling the system.

More precisely, ANN are subsymbolic processing structures that vaguely resemble brain learning operation. They integrate the machine learning algorithms (ML). Information is learned through the connections between inputs and outputs in the nodes (neurons) of the ANN, organized in layers, whose dynamic response is given by external stimuli (adjustment of weights and activation function). The first neural networks that gained massive use were the multilayer perceptron (MLP) networks (de Souza Jr., 1993). More recently, these techniques have evolved to deep learning, in which there are more layers, requiring fewer data pre-processing (LeCun *et al.*, 2015).

Convolutional neural networks (CNNs) have been increasingly used in image processing, solving more efficiently and speedily classification problems (Krizhevsky *et al.*, 2012; LeCun *et al.*, 1989), object detection (Sun *et al.*, 2018), segmentation (Schäfer *et al.*, 2019), and, even, identification of pipeline failures by visual inspection in subsea environments (Petraglia, 2017). CNNs can accommodate the large amount of information coming in the form of tensors, including not only images, but also signal analysis from machinery (Jiao *et al.*, 2020; Zhang *et al.*, 2020; Cheng *et al.*, 2021), spatial and time-domain data transformed (Wu and Zhao, 2018; Ge *et al.*, 2021), acoustic (Wang *et al.*, 2019) and speech recognition (Abdel-Hamid *et al.*, 2014).

In the present era, the industry is entering the fourth industrial revolution, i.e., there is an integration of cyber-physical systems and the advancement of communication and information systems between machines, sensors, and devices. Furthermore, a tremendous amount of process knowledge is collected, enabling the faults detection and diagnosis immediately. Therefore, convolutional neural networks can support the decision-making process, as they are capable of coping the large amounts of image parameters (pixels) and extracting their features, outperforming traditional image processing techniques. The aim of this work is to classify and quantify simulated oil leakage employing convolutional neural network, an innovation in the field of FDD. This paper is divided as follows: how the investigation was developed, including evaluation metrics and the models used are presented on Section 2, results obtained from the experiments are discussed on Section 3. Finally, Section 4 closes it with conclusions and future perspectives.

2. METHODOLOGY

2.1 Computational Fluid Dynamics

Computational Fluid Dynamics were employed by means of the ANSYS Fluent software (Moreira and Bento, 2020). A reduction model was chosen to describe the conditions using a 40 cm height water column and cropping 20 cm of width as seen in Fig. 1. This step aimed to evaluate the two-phase flow (water and air) by air bubbles in different velocities v and different pipelines crack diameters d as seen in Tab. 1. Air was used to validate an experimental reduction model.

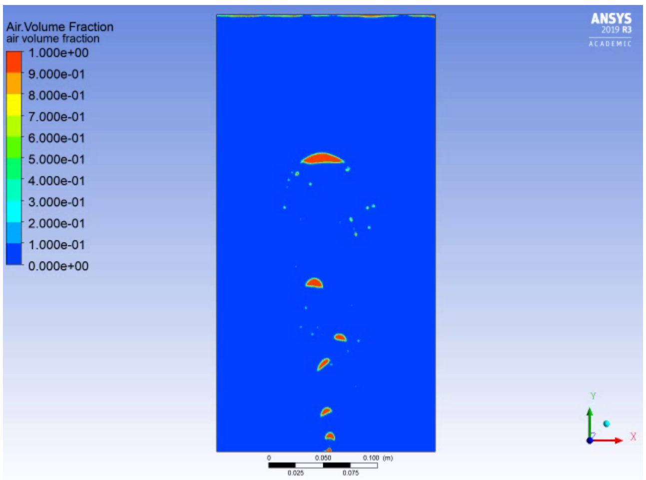

Figure 1: Water column simulated in ANSYS Fluent.

2.2 Convolutional Neural Network used for Classification

The different operational conditions generated a series of videos, which is a visual representation of the phenomena occurring in the reduction model, e.g. the numeric diameter d_b represented in Tab. 1 and in Fig. 1. This series of videos

Table 1: Leakage parameters.

Condition #	d (mm)	v (m/s)	d_b (mm)
1	0.5	0.25	6.45
2		0.63	7.22
3		1.0	7.69
4	1.0	0.24	6.37
5		0.37	6.46
6		0.50	7.28
7	5.0	0.02	6.70
8		0.06	8.05
9		0.09	8.11

were cropped and automatic snapshots using VLC Video Player were taken in order to feed image processing tools and neural networks. Since video had frame ratio of 30 frame per second, but different durations, differente recording ratio were used in order to maintain an uniform dataset as described in Tab. 2. A total number of 3409 images of size 48 x 128 pixels were generated. Starting at the height 18 mm of the water column, the area examined comprised 43 mm x 116 mm in the real scale. A recording ratio is defined as the ratio in which the frame is taken. When recording ratio is equal to one, all frames are captured. On the other hand, when the recording ratio is equal to three, one out of three frames are captured.

Table 2: Video and dataset specifications.

Condition #	Video duration	Recording ratio	Number of images generated
1	00:00:49	3	394
2	00:00:16	1	394
3	00:00:16	1	395
4	00:00:13	1	330
5	00:00:13	1	329
6	00:00:16	1	395
7	00:00:17	1	425
8	00:00:41	3	332
9	00:00:17	1	414

Due to the transient feature of the videos, there is no bubble present at the scene, the leakage takes some seconds to begin. For that reason, a classification network was developed to distinguish between a scenario of normality (no leakage/bubble), abnormal (leakage/bubble). The idea behind is to develop a tool to diagnose any fault in the pipelines.To train the neural network prediction model, it is necessary to define a target, in this case, presence (in binary classification: one) or absence (zero). Images were imported into grayscale using scikit-image processing library (Buitinck *et al.*, 2013). No data pre-processing was necessary to be done, except scaling the input according to the following equation:

$$x' = \frac{x}{255} \tag{1}$$

Next step is to split randomly the dataset into train, validation and test. Train set is used to fit and adjust the weights, and the model is submitted to evaluation using validation set while adjusting the hyperparameters. As the fit process develops, both become biased, therefore is necessary to check the robustness of the model against the test set at the end, which was held during training. Here the proportion adopted was 60 %, 24 % and 16 %, respectively.

This data was fed to Convolutional Neural Network developed in Keras environment using Python, backended by Tensorflow. The architecture employed two convolutional layers, as expressed on Tab. 3. It should be noted that both convolutional layers have kernel size of 3 x 3 and L2 kernel regularizer factor of 0.01, in which the first have 32 filters and the second, 64 filters. Pooling Layers have size 2 x 2 with stride 2.

The units employing activation function uses the rectified linear unit - ReLU (Eq. 2a) and the sigmoid function (Eq. 2b). ReLU increases computational efficiency because it is less subject to the vanishing gradient problem (Glorot *et al.*). The output of a sigmoidal activation is restrict to the range of 0 to 1, representing a probability score. It maps the event of fault occurrence according to the value output, if it is more than 50 %, than the event is classified as abnormal situation (bubble).

Table 3: Classifier CNN architecture.

Layer (type)	Output Shape	Number of parameters
Input	(128, 48, 1)	-
Convolutional 2D + ReLU	(126, 46, 32)	320
Max Pooling 2D	(63, 23, 32)	0
Batch Normalization	(63, 23, 32)	128
Convolutional 2D + ReLU	(126, 46, 32)	18496
Max Pooling 2D	(30, 10, 64)	0
Flatten	(19200)	0
Dropout 20 %	(19200)	0
Dense Layer 1 + ReLU	(16)	307216
Dense Layer 2 + Sigmoid	(1)	17
	Total	326,113 trainable+ 64 non-trainable

$$\mathrm{ReLU(x)} = max(0, x) \tag{2a}$$

$$\mathrm{S(x)} = \frac{1}{1 + e^{-x}} \tag{2b}$$

As loss to be minimized, the average binary cross-entropy for N samples was employed (Eq. 3a). In this notation, q represent the estimated probability, and p the true probability for each class c. Setting the notation as y and $\hat{y}$ for the true and predict outputs, respectively, for a binary case: $p \in \{y, 1-y\}$ and $q \in \{\hat{y}, 1-\hat{y}\}$

Besides the latter, accuracy was also monitored as a metric (Eq. 3b), where the rate of true positives and true negatives over the total number of samples is computed. The optimizer used was Adam. Batch size corresponds to 128 and the maximum number of epoches allowed is equal to 100.

$$\mathrm{CE(p, q)} = -\frac{1}{N}\sum_{n=1}^{N}\sum_{c} p_{n,c}\log q_{n,c} \;= -\frac{1}{N}\sum_{n=1}^{N}[y_n \log \hat{y_n} + (1-y_n)\log(1-\hat{y_n})] \tag{3a}$$

$$\mathrm{ACC} = \frac{1}{N}\sum_{n=1}^{N}[\hat{y_n} == y_n] \tag{3b}$$

3. RESULTS AND DISCUSSION

3.1 CFD Model

3.2 Classifier CNN

A straightforward manner to assess classification is the confusion matrix, illustrated for each data set (Fig. 2). In a binary classification problem, there are four possible outcomes: if the input is positive for bubble presence and the algorithm regards it as positive, then it is denoted as true positive (TP); if there is no bubble on the image and the output is also negative, this is called true negative (TN); if the data is positive, but the prediction is negative, it is a false negative (FN); conversely, it is a false positive (FP) (Tharwat, 2020; Sokolova and Lapalme, 2009). No false positives reported indicates that the classifier does not generate false alarms (or fall-outs) in none of the sets. Also, it is an evidence for the CNN's high specificity (TN rate) and precision. For the FDD, this fact brings reliability to the operator, who would immeaditely recognize the need of taking further actions.

Furthermore, this network possesses a high sensitivity (or recall) regarding the positive detection, with a miss rate of only 0.2 %. Hence, it can be affirmed that this classifier network has a good predictability regarding bubble detection. Investigating the false negatives (Fig. 3) gives an indication of the CNN's capacity. The missed detection in training was due to the choice of assigning an image as "with bubble" as soon the leakage shows off. Thereby a very small piece of bubble was missed out to the neural network.

The progress of the neural network during the epochs is shown at Fig. 4. A fast decrease of both validation and training loss can be seen during the first twenty epochs, while the algorithm converges only after one-hundred iteration

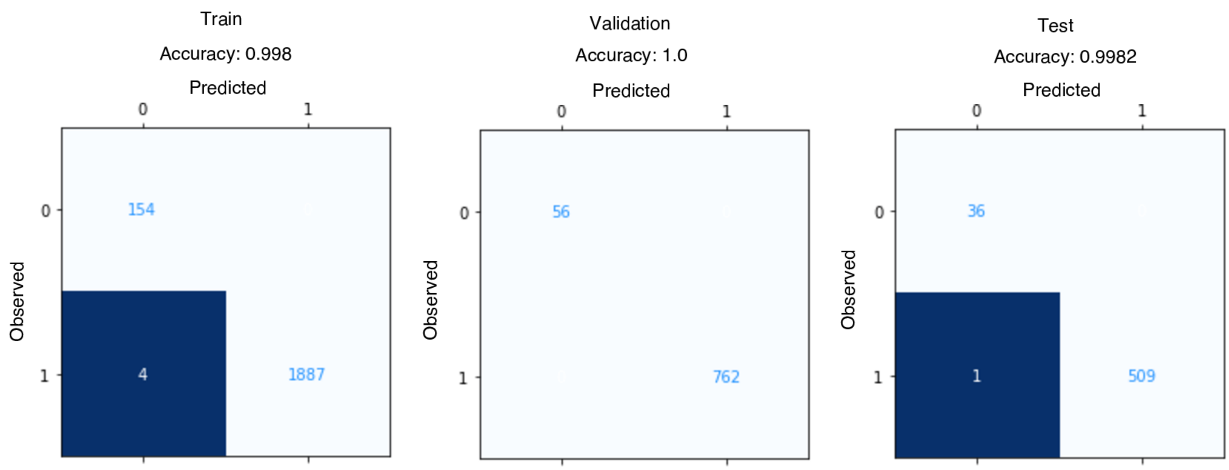

Figure 2: Confusion Matrices.

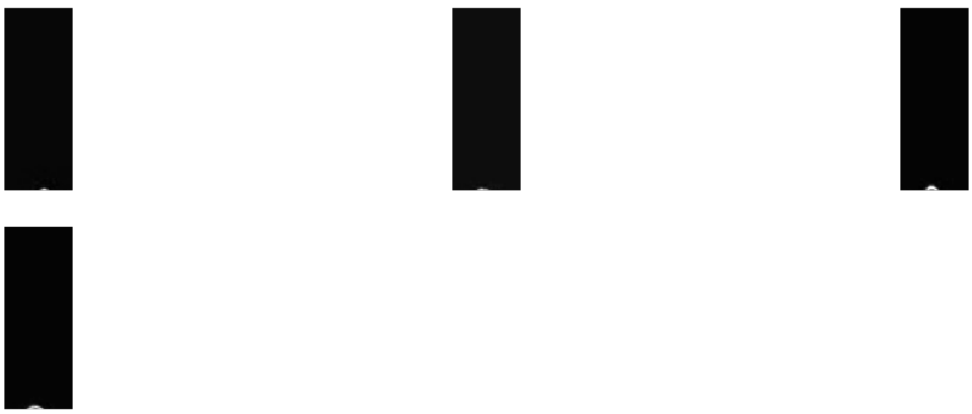

Figure 3: Incorrect predictions from training.

(maximum number set). As the patience adopted was 1.0 x 10^{-4}, the analysis took more time (around twenty minutes) than if softer conditions were applied, which it would probably stopped early. There is, therefore, a clear trade-off between computational time and accuracy.

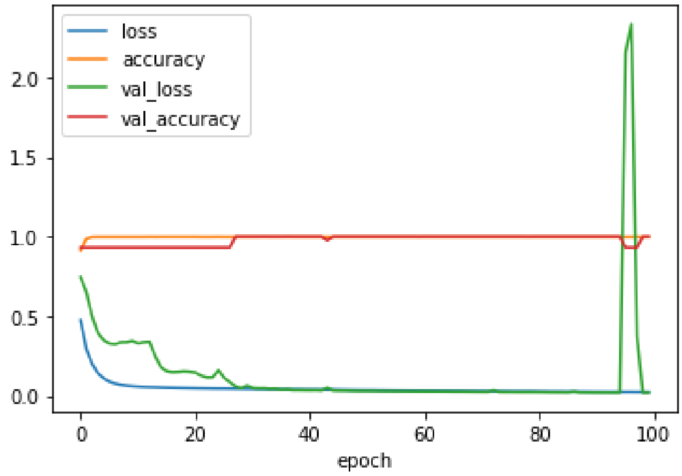

Figure 4: Classifier CNN: Loss and metrics against the epochs.

4. CONCLUSION

A novel methodology using deep learning was presented, combining a classifier and an instance segmentation tool. The classifier provides precise and sensible computational vision, and it is capable of differentiating between images with and without bubbles. Good accuracy supports it as a potential fault detector. It could be extended to other applications in the field of Fault Detection and Diagnosis, not only limiting to this scope.

For future works, the simulation could be broadened to different oil leakage scenarios, but still within minor leak events, since the concept is to work on the prevention of the leak worsening rather than remediation. As a continuation of this work, it is suggested to process experimental data in order to validate the methodology.

5. ACKNOWLEDGEMENTS

The authors acknowledge the financial support granted by the National Agency of Petroleum, Natural Gas, and Biofuels – ANP through the Program of Human Resources for the Oil and Gas Industry (PRH).

6. REFERENCES

Abdel-Hamid, O., Mohamed, A.r., Jiang, H., Deng, L., Penn, G. and Yu, D., 2014. “Convolutional Neural Networks for Speech Recognition”. *IEEE/ACM Transactions on Audio, Speech, and Language Processing*, Vol. 22, No. 10, pp. 1533–1545. ISSN 2329-9290, 2329-9304. doi:10.1109/TASLP.2014.2339736. URL `http://ieeexplore.ieee.org/document/6857341/`.

Buitinck, L., Louppe, G., Blondel, M., Pedregosa, F., Mueller, A., Grisel, O., Niculae, V., Prettenhofer, P., Gramfort, A., Grobler, J., Layton, R., Vanderplas, J., Joly, A., Holt, B. and Varoquaux, G., 2013. “API design for machine learning software: experiences from the scikit-learn project”. *arXiv:1309.0238 [cs]*. URL `http://arxiv.org/abs/1309.0238`. ArXiv: 1309.0238.

Cheng, Y., Lin, M., Wu, J., Zhu, H. and Shao, X., 2021. “Intelligent fault diagnosis of rotating machinery based on continuous wavelet transform-local binary convolutional neural network”. *Knowledge-Based Systems*, Vol. 216, p. 106796. ISSN 09507051. doi:10.1016/j.knosys.2021.106796. URL `https://linkinghub.elsevier.com/retrieve/pii/S0950705121000599`.

Chiang, L.H., Braatz, R.D. and Russell, E., 2001. *Fault detection and diagnosis in industrial systems*. Advanced textbooks in control and signal processing. Springer, London ; New York. ISBN 978-1-85233-327-0.

de Souza Jr., M.B., 1993. *Redes Neuronais Multicamadas Aplicadas a Modelagem e Controle de Processos Químicos.* Tese de Doutorado, PEQ/COPPE/Universidade Federal do Rio de Janeiro, Rio de Janeiro.

Ge, X., Wang, B., Yang, X., Pan, Y., Liu, B. and Liu, B., 2021. “Fault detection and diagnosis for reactive distillation based on convolutional neural network”. *Computers & Chemical Engineering*, Vol. 145, p. 107172. ISSN 00981354. doi:10.1016/j.compchemeng.2020.107172. URL `https://linkinghub.elsevier.com/retrieve/pii/S0098135420309741`.

Glorot, X., Bordes, A. and Bengio, Y., ???? "Deep Sparse Rectifier Neural Networks". p. 9.

Isermann, R., 2006. *Fault-diagnosis systems: an introduction from fault detection to fault tolerance*. Springer, Berlin ; New York. ISBN 978-3-540-24112-6. OCLC: ocm61703226.

Jiao, J., Zhao, M., Lin, J. and Liang, K., 2020. "A comprehensive review on convolutional neural network in machine fault diagnosis". *Neurocomputing*, Vol. 417, pp. 36–63. ISSN 09252312. doi:10.1016/j.neucom.2020.07.088. URL `https://linkinghub.elsevier.com/retrieve/pii/S092523122031225X`.

Krizhevsky, A., Sutskever, I. and Hinton, G.E., 2012. "ImageNet Classification with Deep Convolutional Neural Networks". *Advances in Neural Information Processing Systems*, Vol. 25, pp. 1097–1105. URL `https://proceedings.neurips.cc/paper/2012/hash/c399862d3b9d6b76c8436e924a68c45b-Abstract.html`.

LeCun, Y., Boser, B., Denker, J.S., Henderson, D., Howard, R.E., Hubbard, W. and Jackel, L.D., 1989. "Backpropagation applied to handwritten zip code recognition". *Neural Computation*, Vol. 1, No. 4, pp. 541–551. ISSN 0899-7667. doi:10.1162/neco.1989.1.4.541. URL `https://doi.org/10.1162/neco.1989.1.4.541`.

LeCun, Y., Bengio, Y. and Hinton, G., 2015. "Deep learning". *Nature*, Vol. 521, No. 7553, pp. 436–444. ISSN 1476-4687. doi:10.1038/nature14539. URL `https://www.nature.com/articles/nature14539`. Number: 7553 Publisher: Nature Publishing Group.

Moreira, R. and Bento, T., 2020. "Desenvolvimento e Aplicação de Técnicas de Análise Hidrodinâmica para Quantificação e Avaliação de Vazamentos Subsea a Partir de Imagens". Technical Report PETROBRAS-UFF-FEC 5850.0108939.18.9 SIGITEC-2017/00647-5 PT-143.01.13311 SAP-4600579358, Universidade Federal Fluminense, Niterói.

Nazir, M., Khan, F., Amyotte, P. and Sadiq, R., 2008. "Subsea Release of Oil from a Riser: An Ecological Risk Assessment". *Risk Analysis*, Vol. 28, No. 5, pp. 1173–1196. ISSN 1539-6924. doi:https://doi.org/10.1111/j.1539-6924.2008.01136.x. URL `https://onlinelibrary.wiley.com/doi/abs/10.1111/j.1539-6924.2008.01136.x`. _eprint: https://onlinelibrary.wiley.com/doi/pdf/10.1111/j.1539-6924.2008.01136.x.

Olsen, J.E. and Skjetne, P., 2016. "Current understanding of subsea gas release: A review". *The Canadian Journal of Chemical Engineering*, Vol. 94, No. 2, pp. 209–219. ISSN 00084034. doi:10.1002/cjce.22345. URL `http://doi.wiley.com/10.1002/cjce.22345`.

Petraglia, F., 2017. *Classification of Underwater Pipeline Events using Deep Convolutional NeuralNetworks*. Ph.D. thesis, COPPE/Universidade Federal do Rio de Janeiro, Rio de Janeiro.

Schäfer, J., Schmitt, P., Hlawitschka, M.W. and Bart, H., 2019. "Measuring Particle Size Distributions in Multiphase Flows Using a Convolutional Neural Network". *Chemie Ingenieur Technik*, Vol. 91, No. 11, pp. 1688–1695. ISSN 0009-286X, 1522-2640. doi:10.1002/cite.201900099. URL `https://onlinelibrary.wiley.com/doi/10.1002/cite.201900099`.

Sokolova, M. and Lapalme, G., 2009. "A systematic analysis of performance measures for classification tasks". *Information Processing & Management*, Vol. 45, No. 4, pp. 427–437. ISSN 03064573. doi:10.1016/j.ipm.2009.03.002. URL `https://linkinghub.elsevier.com/retrieve/pii/S0306457309000259`.

Sun, X., Shi, J., Liu, L., Dong, J., Plant, C., Wang, X. and Zhou, H., 2018. "Transferring deep knowledge for object recognition in Low-quality underwater videos". *Neurocomputing*, Vol. 275, pp. 897–908. ISSN 0925-2312. doi:10.1016/j.neucom.2017.09.044. URL `http://www.sciencedirect.com/science/article/pii/S0925231217315631`.

Tharwat, A., 2020. "Classification assessment methods". *Applied Computing and Informatics*, Vol. ahead-of-print, No. ahead-of-print. ISSN 2634-1964, 2210-8327. doi:10.1016/j.aci.2018.08.003. URL `https://www.emerald.com/insight/content/doi/10.1016/j.aci.2018.08.003/full/html`.

Venkatasubramanian, V., Rengaswamy, R. and Kavuri, S.N., 2003a. "A review of process fault detection and diagnosis". *Computers & Chemical Engineering*, Vol. 27, No. 3, pp. 313–326. ISSN 00981354. doi:10.1016/S0098-1354(02)00161-8. URL `https://linkinghub.elsevier.com/retrieve/pii/S0098135402001618`.

Venkatasubramanian, V., Rengaswamy, R., Kavuri, S.N. and Yin, K., 2003b. "A review of process fault detection and diagnosis". *Computers & Chemical Engineering*, Vol. 27, No. 3, pp. 327–346. ISSN 00981354. doi:10.1016/S0098-1354(02)00162-X. URL `https://linkinghub.elsevier.com/retrieve/pii/S009813540200162X`.

Venkatasubramanian, V., Rengaswamy, R., Yin, K. and Kavuri, S.N., 2003c. "A review of process fault detection and diagnosis". *Computers & Chemical Engineering*, Vol. 27, No. 3, pp. 293–311. ISSN 00981354. doi:10.1016/S0098-1354(02)00160-6. URL `https://linkinghub.elsevier.com/retrieve/pii/S0098135402001606`.

Wang, X., Jiao, J., Yin, J., Zhao, W., Han, X. and Sun, B., 2019. "Underwater sonar image classification using adaptive weights convolutional neural network". *Applied Acoustics*, Vol. 146, pp. 145–154. ISSN 0003682X. doi:10.1016/j.apacoust.2018.11.003. URL `https://linkinghub.elsevier.com/retrieve/pii/S0003682X17311532`.

Wu, H. and Zhao, J., 2018. "Deep convolutional neural network model based chemical process fault diagnosis". *Computers & Chemical Engineering*, Vol. 115, pp. 185–197. ISSN 00981354. doi:10.1016/j.compchemeng.2018.04.009.

URL https://linkinghub.elsevier.com/retrieve/pii/S0098135418302990.

Zhang, J., Sun, Y., Guo, L., Gao, H., Hong, X. and Song, H., 2020. "A new bearing fault diagnosis method based on modified convolutional neural networks". *Chinese Journal of Aeronautics*, Vol. 33, No. 2, pp. 439–447. ISSN 10009361. doi:10.1016/j.cja.2019.07.011. URL https://linkinghub.elsevier.com/retrieve/pii/S100093611930278X.

7. RESPONSIBILITY NOTICE

The authors are solely responsible for the printed material included in this paper.